PROCEEDINGS A

The five-dimensional parameter space of grain boundaries

Journal:	*Proceedings A*
Manuscript ID:	RSPA-2015-0442.R1
Article Type:	Research
Date Submitted by the Author:	n/a
Complete List of Authors:	Sutton, Adrian; Imperial College London, Banks, Eliot; Imperial College London, Physics Warwick, Andrew; Imperial College London, Physics
Subject:	Materials science < ENGINEERING AND TECHNOLOGY, Solid state physics < PHYSICS
Keywords:	grain boundaries, metric, crystal symmetry, geodesics, microstructure, Rodrigues vectors

rspa.royalsocietypublishing.org

Research

Article submitted to journal

Subject Areas:
materials science

Keywords:
grain boundaries, metric, geodesics, crystal symmetry, microstructure, Rodrigues vectors

Author for correspondence:
Adrian Sutton
e-mail: a.sutton@imperial.ac.uk

The five-dimensional parameter space of grain boundaries

A P Sutton, E P Banks and A R Warwick

Department of Physics, Imperial College London, Exhibition Road, London SW7 2AZ

To specify a grain boundary at a macroscopic length scale requires the specification of five degrees of freedom. We use a specification in which three degrees of freedom associated with the boundary misorientation are in an orthogonal subspace from two associated with the mean boundary plane. By using Rodrigues vectors to describe rotations we show how paths through these subspaces may be characterized. Some of these paths correspond to physical processes involving grain boundaries during microstructural evolution. Exploiting the orthogonality of the subspaces, a metric to measure 'distance' between two boundaries is defined in terms of the minimum set of rotations required to map one boundary on to the other. We compare our metric with others that have appeared. The existence of rotational symmetry in face-centred cubic crystals leads to as many as 2,304 equivalent specifications of a boundary. We illustrate this multiplicity of descriptions for the (111) twin and a more general boundary. We present an algorithm to evaluate the geodesic distance between two boundaries, and apply it to identify the path along which the distance between these two boundaries is minimized. In general the shortest path does not involve descriptions of boundary misorientations with the smallest misorientation angles.

1. Introduction

Crystalline matter almost always exists in a polycrystalline state comprising an agglomeration of many misoriented but otherwise identical crystals or 'grains'. The interfaces between the crystals are called grain boundaries. They are planar defects on either side of which the orientation of the crystal lattice changes. Grain boundaries play central roles in many properties of crystalline materials [1]. In this paper we attempt to quantify the similarities between different grain boundaries in terms of the parameters used to characterise them. We also explore the shortest paths in this parameter space needed to transform one boundary into another.

In non-enantiomorphic crystals a grain boundary is characterised by five degrees of freedom, which may be specified in several equivalent ways [1]. Following ref. [1] we choose the three variables required to specify the rotation describing the misorientation between the crystal lattices, and the two variables associated with specifying the normal to the boundary plane. In this way the boundary is defined at a macroscopic length scale. At an atomic length scale length there are many more degrees of freedom associated with the atomic structure of a boundary, about which we will say no more here.

One of the most interesting features of grain boundaries is their ability to migrate. For example during recrystallisation they move through deformed regions where they change the crystal orientation and reduce the content of defects, softening the material. The varying mobility of different boundaries may result in a recrystallisation texture, where certain grain orientations are dominant, altering the isotropy of mechanical properties of the material.

In general, as grain boundaries move and absorb other crystal defects their five degrees of freedom change. For example, in recrystallisation small angle grain boundaries may eventually become large angle grain boundaries, whereupon their mobility may increase significantly. Grain boundaries may undergo faceting transitions where the boundary plane changes locally at a fixed crystal misorientation. A graphic example of grain boundaries moving through the five-dimensional space that characterises them is Gleiter's rotating-spheres-on-a-plate experiment [2]. In these experiments a large number of small single crystal copper spheres were placed randomly on a flat single crystal copper substrate and the entire assembly was annealed. During the anneal a neck developed between each sphere and the substrate through diffusion. Inside the neck there was a grain boundary because in general the crystal lattices of the sphere and the substrate had different orientations. The spheres rotated in order to reduce the energy of the grain boundaries in the necks. At the same time the degrees of freedom of the boundaries changed in such a way that the boundary normal remained roughly parallel to the single crystal substrate normal on one side [3].

The changes in the five degrees of freedom associated with the boundaries during these processes may be mapped onto paths in the five-dimensional space used to characterise them. In this paper we consider a representation of the five degrees of freedom entirely in terms of vectors, because it enables paths to be calculated and visualised. It also enables us to define a 'distance' between two grain boundaries in this five-dimensional space. We define the distance as the minimum angle associated with rotations required to transform the five degrees of freedom associated with the first boundary into those of the second. The concept of a distance is useful for interpolating non-singular grain boundary properties, such as self-diffusivity and propensity for segregation of impurities, throughout the five-dimensional space in terms of the known properties at certain points in the space.

The paper is organised as follows. In section 2 we review Frank's median lattice which enables a single coordinate system to be used for both crystals. This section also reviews the concept of the mean boundary plane, and the Rodrigues vector to describe the misorientation between the crystals. The simple formula [1] for determining the boundary plane normals in terms of them is also reviewed. In section 3 we present two geometrical constructions that help the five-dimensional space of grain boundaries to be visualised. The metric for the distance between points in the five-dimensional space is introduced in section 4, and two significant

geodesics through the space are defined. This metric is compared with others in the literature in section 5. When the point group of the crystal includes rotational symmetries there are equivalent descriptions of the boundary in terms of the misorientation and the boundary plane. This complicates the task of defining shortest paths considerably, as discussed in section 6. We conclude in section 7.

2. Frank's median lattice and the mean boundary plane

Frank introduced [4] the concept of the median lattice to simplify expressions for the dislocation content of grain boundaries. Sutton and Balluffi [1] showed that it is also a useful concept in the characterisation of a grain boundary. Although there are two misoriented crystals that meet at the grain boundary, each with its own coordinate system, the use of the median lattice enables just *one* coordinate system to be used for *both* crystals.

The median lattice is a single crystal lattice. Let $\hat{\mathbf{n}}$ and $\hat{\mathbf{n}}'$ be normal to two planes in this lattice. We choose to express these vectors in the coordinate system of the median lattice. One crystal lattice that meets at the grain boundary is generated by applying to the median lattice a rotation of $+\theta/2$ about an axis $\hat{\boldsymbol{\rho}}$, and the other by applying to the median lattice in its original orientation a rotation of $-\theta/2$ about an axis $\hat{\boldsymbol{\rho}}$. The final misorientation angle between the two crystal lattices is θ. During these rotations the vectors normal to planes in each crystal are rotated along with the crystal lattices, but their components remain as they were in the median lattice. If the two vectors $\hat{\mathbf{n}}$ and $\hat{\mathbf{n}}'$ are now parallel they can be normal to a grain boundary plane. The components of $\hat{\mathbf{n}}$ and $\hat{\mathbf{n}}'$ will differ unless they are parallel to the rotation aixs. In this way the vectors normal to a boundary plane in the two crystal lattices are expressed in the coordinate system of a single lattice, the median lattice. The construction process is illustrated schematically in figure 1.

Let the misorientation between the crystal lattices be represented by the Rodrigues vector $\boldsymbol{\rho} = \hat{\boldsymbol{\rho}} \tan\theta/2$. If $\mathbf{n}$ and $\mathbf{n}'$ are parallel to the boundary plane normal in the two crystal lattices then Sutton and Balluffi showed ([1], p.22) that:

$$\mathbf{n} = \mathbf{N} - \mathbf{N} \times \boldsymbol{\rho} \tag{2.1}$$

$$\mathbf{n}' = \mathbf{N} + \mathbf{N} \times \boldsymbol{\rho} \tag{2.2}$$

We note that interchanging $\mathbf{n}$ and $\mathbf{n}'$ does not produce a distinct grain boundary. This is effected by changing the sign of $\boldsymbol{\rho}$, which may be realised by reversing the direction of the rotation axis $\hat{\boldsymbol{\rho}}$. $\mathbf{N}$ is called the mean boundary plane normal because $\mathbf{N} = (\mathbf{n} + \mathbf{n}')/2$. As the misorientation angle θ tends to zero, $\mathbf{n}$ and $\mathbf{n}'$ tend to $\mathbf{N}$. The mean boundary plane is therefore a plane in the median lattice to which the grain boundary is related by applying equal and opposite rotations to the median lattice. Figure 2 illustrates these features.

In equations 2.1 and 2.2 the mean boundary plane does not change direction if both equations are multiplied by the same scalar quantity. Thus, $|\mathbf{N}|$ is arbitrary because it affects only the magnitudes $|\mathbf{n}|$ and $|\mathbf{n}'|$. But it is clear that if $\mathbf{N}$ and $\boldsymbol{\rho}$ are both rational then so are $\mathbf{n}$ and $\mathbf{n}'$ (see ref [1], p.22): rational grain boundaries are generated from rational mean boundary planes and rational Rodrigues vectors. This is particularly significant in cubic crystals because all coincidence site lattices are generated by rational Rodrigues vectors.

The arbitrary magnitude of $|\mathbf{N}|$ is a consequence of the fact that only the direction of $\mathbf{N}$ in equations 2.1 and 2.2 matters. There are three degrees of freedom associated with the Rodrigues vector, $\boldsymbol{\rho} = \hat{\boldsymbol{\rho}} \tan\theta/2$, and there are two further, independent degrees of freedom associated with the direction of $\mathbf{N}$. Thus we account for the five degrees of freedom associated with a grain boundary.

By fixing $\mathbf{N}$ and $\hat{\boldsymbol{\rho}}$ and allowing θ to vary we generate a systematic series of grain boundaries, all sharing the same mean boundary plane and rotation axis, where only the misorientation angle varies. For example, in a cubic crystal with $\mathbf{N} = [110]$ and $\boldsymbol{\rho} = \frac{p}{q}[001]$, where p and q are integers

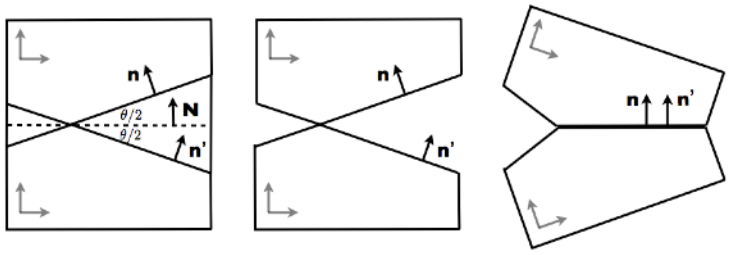

Figure 1. To illustrate the construction of a grain boundary from the median lattice. On the left we start with a single crystal lattice, called the median lattice. A lattice plane (broken line) with normal $\mathbf{N}$ is selected, which will become the location of the boundary. This is the mean boundary plane. We identify two further lattice planes with normals $\mathbf{n}$ and $\mathbf{n}'$ at $\pm\theta/2$ on either side of the mean boundary plane. These will become the plane normals of the grain boundary. In the centre image the material between the planes with normals $\mathbf{n}$ and $\mathbf{n}'$ is removed to enable the crystal halves to be rotated. On the right the upper crystal is rotated by $\theta/2$ clockwise and the lower crystal by $\theta/2$ counterclockwise, so the two crystal halves meet forming a grain boundary with misorientation angle θ and normals $\mathbf{n}$ and $\mathbf{n}'$. *Both* the coordinate system and the vectors in each crystal are rotated. As a result $\mathbf{n}+\mathbf{n}'$ remains parallel to $\mathbf{N}$ throughout the construction. In this illustration the rotation axis is perpendicular to the page for simplicity. In general it is inclined to the page. After refs. [5] and [6].

and $\frac{p}{q}=\tan(\theta/2)$, we generate the familiar series of symmetric $[001]$ tilt boundaries: $\mathbf{n}=[q-p,\ q+p,\ 0]$ and $\mathbf{n}'=[q+p,\ q-p,\ 0]$.

Equations 2.1 and 2.2 also enable all possible grain boundary normals with a given misorientation $\boldsymbol{\rho}$ to be generated by allowing $\mathbf{N}$ to range over all normals to planes of the median lattice. This generates the normals to all possible boundary planes of a misoriented crystal embedded within another crystal. For example, for $\boldsymbol{\rho}=\frac{1}{3}[111]$ in a cubic crystal, which generates the $\Sigma=3$ coincidence site lattice[1], and $\mathbf{N}=[HKL]$, we generate boundary plane normals $\mathbf{n}=[3H+L-K,\ 3K+H-L,\ 3L+K-H]$ and $\mathbf{n}'=[3H-L+K,\ 3K-H+L,\ 3L-K+H]$. Alternatively, as we shall see later, we may choose to represent this crystal misorientation by $\boldsymbol{\rho}=\frac{1}{2}[101]$. The boundary plane normals with $\mathbf{N}=[HKL]$ then become $\mathbf{n}=[2H-K,\ 2K-L+H,\ 2L+K]$ and $\mathbf{n}'=[2H+K,\ 2K+L-H,\ 2L-K]$. This illustrates an important point: in general, equivalent descriptions of the crystal misorientation and the *same* mean boundary plane generate *different* boundary normals in equations 2.1 and 2.2.

The remarkable formula [7] for combining Rodrigues vectors is as follows:

$$\boldsymbol{\rho}_2\star\boldsymbol{\rho}_1=\frac{\boldsymbol{\rho}_1+\boldsymbol{\rho}_2-\boldsymbol{\rho}_1\times\boldsymbol{\rho}_2}{1-\boldsymbol{\rho}_1\cdot\boldsymbol{\rho}_2}, \tag{2.3}$$

[1]If the lattices of two misoriented crystals are allowed to interpenetrate there are certain misorientations where a superlattice exists of coincident sites common to both crystal lattices. The superlattice is called a coincidence site lattice and the ratio of the number of sites of one crystal lattice to the number of coincident sites is called Σ

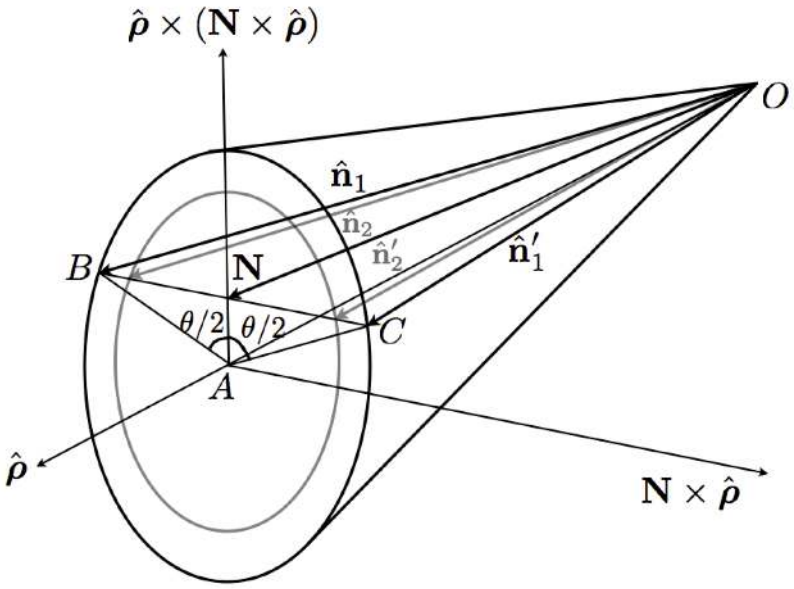

Figure 2. The geometry of equations 2.1 and 2.2. The rotation axis $\hat{\boldsymbol{\rho}}$ is inclined to the mean boundary plane $\mathbf{N}$. The unit normals to the boundary of misorientation θ about $\hat{\boldsymbol{\rho}}$ are the vectors $\hat{\mathbf{n}}_1$ and $\hat{\mathbf{n}}'_1$, shown as black arrows. Note that $\mathbf{N}$ is parallel to $\hat{\mathbf{n}}_1 + \hat{\mathbf{n}}'_1$. The length of BC is $2|\mathbf{N} \times \hat{\boldsymbol{\rho}}|\tan(\theta/2) = 2|\mathbf{N} \times \boldsymbol{\rho}|$. Thus $\hat{\mathbf{n}}_1 = \mathbf{N} - \mathbf{N} \times \boldsymbol{\rho}$ and $\hat{\mathbf{n}}'_1 = \mathbf{N} + \mathbf{N} \times \boldsymbol{\rho}$, which are equations 2.1 and 2.2. The grey arrows show the boundary normals $\hat{\mathbf{n}}_2$ and $\hat{\mathbf{n}}'_2$ when the misorientation angle is decreased. Note that $\mathbf{N}$ remains parallel to $\hat{\mathbf{n}}_2 + \hat{\mathbf{n}}'_2$. As $\theta \to 0$ the boundary normals become coincident with $\mathbf{N}$: the boundary plane becomes a plane of the perfect crystal with normal $\mathbf{N}$. After fig.1.7 of ref. [1].

where $\boldsymbol{\rho}_2 \star \boldsymbol{\rho}_1$ is the Rodrigues vector representing the resultant rotation obtained by first applying the rotation represented by $\boldsymbol{\rho}_1$ followed by the rotation represented by $\boldsymbol{\rho}_2$. We will use this formula extensively in the following[2].

Gibbs[3] [8] showed that we may eliminate $\mathbf{N}$ in equations 2.1 and 2.2 to obtain the relationship between $\hat{\mathbf{n}}$ and $\hat{\mathbf{n}}'$:

$$\begin{aligned} \hat{\mathbf{n}} &= \frac{(1-\rho^2)\hat{\mathbf{n}}' + 2(\boldsymbol{\rho} \cdot \hat{\mathbf{n}}')\boldsymbol{\rho} - 2\hat{\mathbf{n}}' \times \boldsymbol{\rho}}{1+\rho^2} \\ &= \boldsymbol{\rho} \star \hat{\mathbf{n}}' \star (-\boldsymbol{\rho}). \end{aligned} \tag{2.4}$$

The first line of equation 2.4 expresses the relationship between $\mathbf{n}$ and $\mathbf{n}'$ as a rotation in terms of the usual 'rotation formula', e.g. [1] p.9. When this equation is expressed in Cartesian components

[2]This formula is closely related to the formula for combining quaternions, but it was published by Rodrigues in 1840, three years before Hamilton's quaternions.

[3]Gibbs showed that equations 2.1 and 2.2 hold for all vectors $\mathbf{N}$ in that the rotation represented by $\boldsymbol{\rho}$ (which he gave the unmemorable name *a vector semi-tangent of version*) carries $\mathbf{n}'$ into $\mathbf{n}$. By eliminating $\mathbf{N}$ he derived the rotation formula. He also derived equation 2.3. It is not known whether Gibbs was aware of the paper by Rodrigues because he included no references in his lecture notes on vector analysis.

it enables the matrix $\boldsymbol{R}$ representing the grain boundary misorientation to be expressed in terms of the components of the corresponding Rodrigues vector:

$$\mathcal{R}_{ij} = \frac{(1-\rho^2)\delta_{ij} + 2\rho_i\rho_j - 2\epsilon_{ijk}\rho_k}{1+\rho^2},$$

where $n_i = \mathcal{R}_{ij}n'_j$, or $\mathbf{n} = \boldsymbol{R}\mathbf{n}'$. We will not make any further reference to rotation matrices in this paper. The second line of equation 2.4 expresses the rotation *operation* on $\mathbf{n}'$ in terms of Rodrigues vectors, in which $\mathbf{n}'$ is itself treated as a Rodrigues vector. There is a similar formula for rotation operations involving quaternions, e.g. [9].

3. Geometrical constructions

If we choose the grain boundary normals $\mathbf{n}$ and $\mathbf{n}'$ to be unit vectors $\hat{\mathbf{n}}$ and $\hat{\mathbf{n}}'$, then $\mathbf{N}$ has a definite magnitude which depends on $\boldsymbol{\rho}$. The condition that $\hat{\mathbf{n}}$ and $\hat{\mathbf{n}}'$ are unit vectors leads to the following restriction on the length of the vector $\mathbf{N}$ parallel to the mean boundary plane normal:

$$|\mathbf{N}|^2 = \frac{1}{1+\tan^2(\theta/2)\sin^2\alpha}, \tag{3.1}$$

where α is the angle between $\mathbf{N}$ and $\hat{\boldsymbol{\rho}}$. This leads to the construction shown in fig. 3, where the mean boundary plane normal $\mathbf{N}$ in equations 2.1 and 2.2 lies on a prolate spheroid with major axis along $\hat{\boldsymbol{\rho}}$. The semi-major axis is 1 and the semi-minor axis is $\cos(\theta/2)$, so that the eccentricity is $\sin(\theta/2)$. As $\theta \to 0$ the prolate spheroid tends towards a sphere, and the boundary normals $\hat{\mathbf{n}}$ and $\hat{\mathbf{n}}'$ tend to $\mathbf{N}$, which becomes a unit vector. At the other extreme as $\theta \to \pi$ the prolate spheroid tends to the diameter parallel to $\hat{\boldsymbol{\rho}}$.

For a given $\mathbf{N}$ and $\hat{\boldsymbol{\rho}}$ equations 2.1 and 2.2 lead to the construction shown in fig.4. The unit normals $\hat{\mathbf{n}}$ and $\hat{\mathbf{n}}'$ are radius vectors of the sphere. As θ increases $|\mathbf{N} \times \boldsymbol{\rho}|$ increases too, which results in decreasing $|\mathbf{N}|$. By allowing $\hat{\boldsymbol{\rho}}$ to range over all possible radius vectors of the unit sphere, and $\mathbf{N}$ to range over all points within the sphere we may represent the normals $\hat{\mathbf{n}}$ and $\hat{\mathbf{n}}'$ of all possible grain boundary planes in the five-dimensional space. The misorientation angle θ for a given choice of $\mathbf{N}$ and $\hat{\boldsymbol{\rho}}$ follows immediately from equation 3.1. In both constructions there are three degrees of freedom associated with $\mathbf{N}$ and two associated with $\hat{\boldsymbol{\rho}}$, giving five altogether.

In the remainder of this paper the five degrees of freedom of a grain boundary will be the three associated with the Rodrigues vector representing the misorientation relationship between the crystals, and the two associated with the direction of the mean boundary plane.

4. The metric

In this section we define a metric to measure the 'distance' between two boundaries. The distance will be a measure of the extent of the operations required to transform the five degrees of freedom of one boundary into those of the other.

The choice of metric is not unique. There are certain mathematical conditions that have to be satisfied by any metric, which are enumerated below. Assuming those conditions are satisfied the choice has to be motivated by other considerations, such as the physical processes by which grain boundaries alter their five degrees of freedom. The metric we develop in this paper describes the changes in the five degrees of freedom associated with two independent physical processes. Their independence physically is reflected in the independence of $\mathbf{N}$ and $\boldsymbol{\rho}$ mathematically.

The first process is faceting, where the mean boundary plane changes but the misorientation relationship remains constant. The second is where the misorientation relationship changes but the mean boundary plane remains constant. This can be effected in principle by the absorption of dislocations from the adjoining crystal lattices, although in practice such a random process would normally change both the mean boundary plane and the misorientation relationship. But this second process does relate directly to many systematic studies of grain boundaries by computer

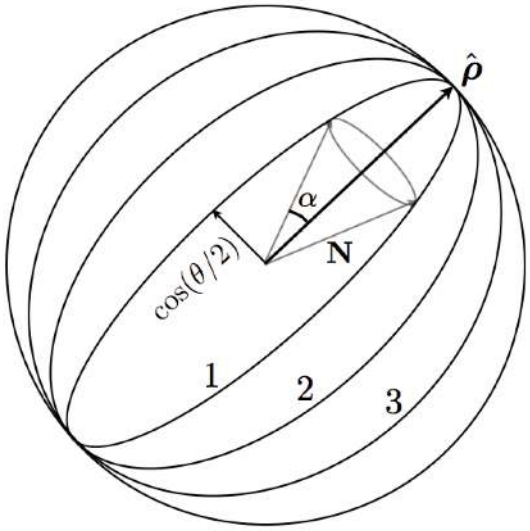

Figure 3. Geometrical construction to illustrate equation 3.1. The normal to the mean boundary plane $\mathbf{N}$ lies on a cone of semi-angle α, with axis $\hat{\boldsymbol{\rho}}$, the rotation axis. As the angle α varies between 0 and π the mean boundary plane normal $\mathbf{N}$ moves on the surface of a prolate spheroid, with semi-minor axis $\cos(\theta/2)$, where θ is the boundary misorientation angle. As θ decreases the prolate spheroid moves from positions 1 to 2 to 3, eventually coinciding with the unit sphere when the misorientation is zero. In the limit that the misorientation is π the prolate spheroid shrinks to the diameter parallel to $\hat{\boldsymbol{\rho}}$.

simulation where the mean boundary plane and misorientation axis are held constant and the misorientation angle is varied, as discussed in section 2.

The independence of these two physical processes implies that the distance between two arbitrary boundaries involves independent contributions arising from the change in the mean boundary plane and the change in the misorientation relationship. A change in the mean boundary plane cannot be effected by a change in the misorientation relationship and *vice versa*. Therefore, we choose to define the distance between the boundaries as the sum of these two contributions.

Consider two grain boundaries labelled '1' and '2'. They are each characterised by a mean boundary plane and a Rodrigues vector: ($\hat{\mathbf{N}}_1$, $\boldsymbol{\rho}_1$) and ($\hat{\mathbf{N}}_2$, $\boldsymbol{\rho}_2$), where $\boldsymbol{\rho}_1 = \hat{\boldsymbol{\rho}}_1 \tan(\theta_1/2)$ and $\boldsymbol{\rho}_2 = \hat{\boldsymbol{\rho}}_2 \tan(\theta_2/2)$. The normals to the boundaries ($\mathbf{n}_1$, $\mathbf{n}_1'$) and ($\mathbf{n}_2$, $\mathbf{n}_2'$) are obtained from ($\hat{\mathbf{N}}_1$, $\boldsymbol{\rho}_1$) and ($\hat{\mathbf{N}}_2$, $\boldsymbol{\rho}_2$) using equations 2.1 and 2.2.

Consider first the case of a very large, spherical, misoriented crystal embedded inside another crystal. The large radius enables the boundary plane to be identified locally. Clearly, the boundaries of the embedded grain share the same misorientation $\boldsymbol{\rho} = \hat{\boldsymbol{\rho}} \tan(\theta/2)$ between the crystals, but they have different mean boundary planes. To transform one boundary surrounding the embedded grain into another we have to change the direction of the mean boundary plane from $\hat{\mathbf{N}}_1$ to $\hat{\mathbf{N}}_2$. This may be achieved through the following sequence of operations: (i) Reverse the rotations of the two crystals by $\pm\theta/2$ about $\hat{\boldsymbol{\rho}}$ to return the embedded crystal to the same orientation as the surrounding crystal. During this operation the location of the boundary with

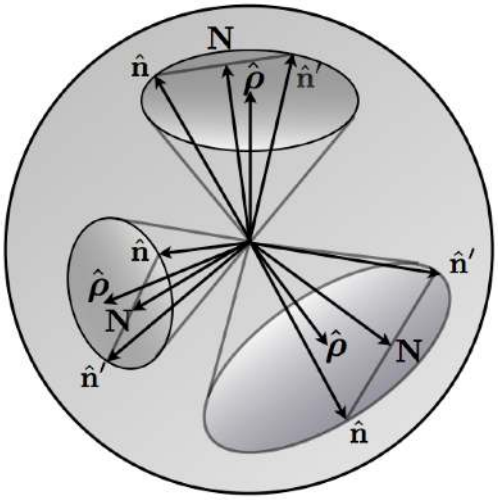

Figure 4. A construction to represent all possible gain boundaries in the 5D parameter space. The rotation axes $\hat{\boldsymbol{\rho}}$ and mean boundary plane normals $\mathbf{N}$ of three grain boundaries are represented by vectors in a unit sphere. $\hat{\boldsymbol{\rho}}$ and $\mathbf{N}$ define the unit boundary normals $\hat{\mathbf{n}}$ and $\hat{\mathbf{n}}'$ as radius vectors of the unit sphere. The boundary normals $\hat{\mathbf{n}}$ and $\hat{\mathbf{n}}'$ lie on a cone with axis $\hat{\boldsymbol{\rho}}$, and apex at the centre of the sphere. The base of the cone is a circle on the surface of the sphere. It is the same cone as depicted in fig.2. By allowing $\hat{\boldsymbol{\rho}}$ to range over all possible radius vectors, and by allowing $\mathbf{N}$ to be any point within the sphere, unit boundary normals of all possible grain boundaries throughout the 5D parameter space may be generated. This construction is based on equations 2.1 and 2.2, but with the requirement that the normals to the boundary plane are unit vectors, which fixes the magnitude of $\mathbf{N}$.

mean boundary plane $\hat{\mathbf{N}}_1$ does not change but the misorientation between the crystal lattices on either side of it decreases to zero. When the angle of misorientation reaches zero the boundary plane becomes a plane in a single crystal with normal $\hat{\mathbf{N}}_1$. (ii) Rotate the entire single crystal to bring the plane with normal $\hat{\mathbf{N}}_2$ into the former location of the plane with normal $\hat{\mathbf{N}}_1$. This involves a rotation of the single crystal by $\psi_{12} = \cos^{-1}(\hat{\mathbf{N}}_1 \cdot \hat{\mathbf{N}}_2)$. This is the step that changes the mean boundary plane normal. (iii) Reintroduce the misorientation between the embedded and surrounding crystals by applying equal and opposite rotations of $\theta/2$ to each crystal about the axis $\hat{\boldsymbol{\rho}}$. At the end of this sequence of operations the boundary $(\hat{\mathbf{N}}_1, \boldsymbol{\rho})$ has been transformed into the boundary $(\hat{\mathbf{N}}_2, \boldsymbol{\rho})$. The rotations in the first and third steps are equal and opposite. The net rotation is the change of the mean boundary plane normal $\hat{\mathbf{N}}$ by $\psi_{12} = \cos^{-1}(\hat{\mathbf{N}}_1 \cdot \hat{\mathbf{N}}_2)$. As $\hat{\mathbf{N}}$ traces the arc of the great circle between $\hat{\mathbf{N}}_1$ and $\hat{\mathbf{N}}_2$ it varies as follows:

$$\hat{\mathbf{N}} = \frac{\sin(\psi_{12} - \psi)\hat{\mathbf{N}}_1 + \sin\psi\hat{\mathbf{N}}_2}{\sin\psi_{12}}, \tag{4.1}$$

where $0 \leq \psi \leq \psi_{12}$. Equation 4.1 is the shortest path connecting $\hat{\mathbf{N}}_1$ and $\hat{\mathbf{N}}_2$ in the two-dimensional subspace associated with mean boundary plane normals.

Now consider the case where the mean boundary plane $\hat{\mathbf{N}}$ does not change but the boundary misorientation changes from that represented by $\boldsymbol{\rho}_1 = \hat{\boldsymbol{\rho}}_1 \tan(\theta_1/2)$ to that represented by $\boldsymbol{\rho}_2 = \hat{\boldsymbol{\rho}}_2 \tan(\theta_2/2)$. Let θ_{12} be the angle associated with the Rodrigues vector $\boldsymbol{\rho}_{1\to 2} = \boldsymbol{\rho}_2 \star (-\boldsymbol{\rho}_1) = \hat{\boldsymbol{\rho}}_{1\to 2} \tan \theta_{12}/2$, representing the rotation required to transform $\boldsymbol{\rho}_1$ into $\boldsymbol{\rho}_2$, thus $\boldsymbol{\rho}_2 = \boldsymbol{\rho}_{1\to 2} \star \boldsymbol{\rho}_1$. This may be achieved by the following two operations: (i) Reverse the rotations of the two crystals by $\pm\theta_1/2$ about $\hat{\boldsymbol{\rho}}_1$ to return the boundary $(\hat{\mathbf{N}}, \boldsymbol{\rho}_1)$ to the plane with normal $\hat{\mathbf{N}}$ in the single crystal. (ii) Apply the rotations $\pm\theta_2/2$ about $\hat{\boldsymbol{\rho}}_2$ to the two crystals to generate the boundary $(\hat{\mathbf{N}}, \boldsymbol{\rho}_2)$. The resultant change of misorientation is given by $\boldsymbol{\rho}_{1\to 2} = \hat{\boldsymbol{\rho}}_{1\to 2} \tan(\theta_{12}/2)$, where

$$\tan^2(\theta_{12}/2) = \frac{(\boldsymbol{\rho}_1 - \boldsymbol{\rho}_2)^2 + (\boldsymbol{\rho}_1 \times \boldsymbol{\rho}_2)^2}{(1 + \boldsymbol{\rho}_1 \cdot \boldsymbol{\rho}_2)^2} = \frac{(1+\boldsymbol{\rho}_1^2)(1+\boldsymbol{\rho}_2^2)}{(1 + \boldsymbol{\rho}_1 \cdot \boldsymbol{\rho}_2)^2} - 1. \tag{4.2}$$

In the general case there is a change of mean boundary plane normal and a change of the misorientation relationship between two crystals. The rotations associated with these changes are independent and in orthogonal subspaces: one does not affect the other. The two rotations may be done in either order to effect the same resultant change of mean boundary plane and misorientation relation. This is evident in equations 2.1 and 2.2 where $\mathbf{N}$ and $\boldsymbol{\rho}$ may be varied independently. It follows that the 'distance' between two boundaries may be defined as follows:

$$\Delta_{12} = \psi_{12} + \theta_{12}, \tag{4.3}$$

where ψ_{12} and θ_{12} are taken as positive. Any change required in ψ_{12} cannot be effected by a change in θ_{12} and *vice versa*. This is because to change ψ_{12} we have to rotate *both* crystals together, to maintain the same relative orientation of the two crystals while changing the mean boundary plane. In contrast a change in θ_{12} involves a change in the relative orientation of the two crystals while maintaining the same mean boundary plane. We note that $\sqrt{\psi_{12}^2 + \theta_{12}^2}$ is always less than $\psi_{12} + \theta_{12}$ provided $\psi_{12} \neq 0$ and $\theta_{12} \neq 0$, and therefore this expression does not capture the full extent of the rotations required to transform one boundary into the other.

Before any crystal point group symmetries are taken into account $0 \leq \psi_{12} \leq \pi/2$[4] and $0 \leq \theta_{12} \leq \pi$, and the maximum value of Δ_{12} is therefore $3\pi/2$. The metric thus defined takes into account differences in both the crystal misorientation and the mean boundary plane.

For the metric in equation 4.3 to be an acceptable measure of the 'distance' between two grain boundaries it must satisfy the following four criteria:

(i) The distance between two grain boundaries must be positive or zero.
(ii) If it is zero then the two grain boundaries are identical with the same Rodrigues vector and the same mean boundary plane.
(iii) The distance between grain boundary 1 and grain boundary 2 must be the same as the distance between grain boundary 2 and grain boundary 1.
(iv) The distance between grain boundaries 1 and 2 must be less than or equal to the sum of the distances between grain boundaries 1 and 3 and grain boundaries 3 and 2, where grain boundary 3 is any other grain boundary. This is known as the triangle inequality. The equality holds when grain boundary 3 lies on the geodesic between grain boundaries 1 and 2.

It is obvious that the first three criteria are satisfied by our metric. Since the Rodrigues vectors and mean boundary plane normals lie in orthogonal subspaces of the 5 dimensional space, it is necessary only to show that the triangle inequality is satisfied in each of these subspaces. The geodesic in the 3D space of Rodrigues vectors between $\boldsymbol{\rho}_1$ and $\boldsymbol{\rho}_2$ is the straight line $(\lambda\boldsymbol{\rho}_{1\to 2}) \star \boldsymbol{\rho}_1 = \lambda(\boldsymbol{\rho}_2 \star (-\boldsymbol{\rho}_1)) \star \boldsymbol{\rho}_1$, where λ varies from 0 to 1:

[4] if $\psi_{12} > \pi/2$ then it may be brought within the range $0 \leq \psi_{12} \leq \pi/2$ by changing the sign of $\mathbf{N}_1$ or $\mathbf{N}_2$.

$$\lambda(\boldsymbol{\rho}_2 \star (-\boldsymbol{\rho}_1)) \star \boldsymbol{\rho}_1 = \boldsymbol{\rho}_1 + \frac{\lambda(1+\boldsymbol{\rho}_1^2)}{1+\boldsymbol{\rho}_1\cdot\boldsymbol{\rho}_2+\lambda(\boldsymbol{\rho}_1^2-\boldsymbol{\rho}_1\cdot\boldsymbol{\rho}_2)}(\boldsymbol{\rho}_2-\boldsymbol{\rho}_1)$$

$$= \boldsymbol{\rho}_1 + f(\lambda)(\boldsymbol{\rho}_2-\boldsymbol{\rho}_1), \tag{4.4}$$

where $f(\lambda)$ is a scalar function of λ satisfying $f(\lambda)=0$ when $\lambda=0$ and $f(\lambda)=1$ when $\lambda=1$. It follows that $\theta_{13}+\theta_{32}\geq\theta_{12}$ and the equality holds only when $\boldsymbol{\rho}_3$ lies on the straight line in equation 4.4 between $\boldsymbol{\rho}_1$ and $\boldsymbol{\rho}_2$.

Turning to the 2D subspace of the mean boundary plane normals, these are radius vectors of the unit sphere. The angle ψ_{12} between $\hat{\mathbf{N}}_1$ and $\hat{\mathbf{N}}_2$ is the length of the arc of the great circle passing through these points on the surface of the unit sphere (see equation 4.1). Consider a third mean boundary plane unit normal $\hat{\mathbf{N}}_3$. Then $\psi_{13}+\psi_{32}\geq\psi_{12}$ and the equality holds when $\hat{\mathbf{N}}_3$ lies on the great circle between $\hat{\mathbf{N}}_1$ and $\hat{\mathbf{N}}_2$.

We conclude that the metric defined in equation 4.3 satisfies the four criteria listed above.

5. Comparisons with the literature

(a) Morawiec (2000)

Morawiec [10] defined a metric as follows:

$$\Delta_{12}^{(M)} = 2\,(1-\cos\theta_{12}) + (1-\hat{\mathbf{n}}_1\cdot\hat{\mathbf{n}}_2) + \left(1-\hat{\mathbf{n}}_1'\cdot\hat{\mathbf{n}}_2'\right) \tag{5.1}$$

The first term on the right of equation 5.1 is the contribution arising from the misorientation of the crystal lattices. It may be expressed in terms of Rodrigues vectors as follows:

$$2\,(1-\cos\theta_{12}) = 4\,\frac{\boldsymbol{\rho}_{1\to2}^2}{1+\boldsymbol{\rho}_{1\to2}^2} = 4\left\{\frac{(\boldsymbol{\rho}_1-\boldsymbol{\rho}_2)^2+(\boldsymbol{\rho}_1\times\boldsymbol{\rho}_2)^2}{(1+\boldsymbol{\rho}_1^2)(1+\boldsymbol{\rho}_2^2)}\right\} \tag{5.2}$$

The second and third terms on the right of equation 5.1 represent the contribution from the changes in boundary normals. Using equations 2.1 and 2.2 they may be expressed as follows:

$$(1-\hat{\mathbf{n}}_1\cdot\hat{\mathbf{n}}_2)+\left(1-\hat{\mathbf{n}}_1'\cdot\hat{\mathbf{n}}_2'\right) = 2\left\{1-\frac{\hat{\mathbf{N}}_1\cdot\hat{\mathbf{N}}_2+\left(\hat{\mathbf{N}}_1\times\boldsymbol{\rho}_1\right)\cdot\left(\hat{\mathbf{N}}_2\times\boldsymbol{\rho}_2\right)}{\left|\hat{\mathbf{N}}_1+\hat{\mathbf{N}}_1\times\boldsymbol{\rho}_1\right|\left|\hat{\mathbf{N}}_2+\hat{\mathbf{N}}_2\times\boldsymbol{\rho}_2\right|}\right\} \tag{5.3}$$

We see that the contribution arising from the boundary normals is not independent of the boundary misorientations because both $\boldsymbol{\rho}_1$ and $\boldsymbol{\rho}_2$ appear on the right hand side. This lack of separation between the contributions from (a) the misorientations of the two crystals and (b) the boundary normals, leads to inconsistencies. For example, if $\hat{\mathbf{N}}_1=\hat{\mathbf{N}}_2$ we have seen that the shortest path connecting the boundaries involves only the change in the misorientation $\boldsymbol{\rho}_{1\to2}$. The change in the boundary normals from $\hat{\mathbf{n}}_1,\hat{\mathbf{n}}_1'$ to $\hat{\mathbf{n}}_2,\hat{\mathbf{n}}_2'$ is effected entirely by replacing $\boldsymbol{\rho}_1$ in equations 2.1 and 2.2 by $\boldsymbol{\rho}_2$. In this case the metric should have *no* contribution from the change in the boundary normals. In equation 4.3 this is indeed the case because $\psi_{12}=0$. But that is clearly not the case in equation 5.3.

Another inconsistency is evident when $\boldsymbol{\rho}_1=\boldsymbol{\rho}_2$ and $\hat{\mathbf{N}}_1\neq\hat{\mathbf{N}}_2$. This describes two boundaries with the same misorientation relationship but different planes. The metric should then be independent of $\boldsymbol{\rho}_1$ and $\boldsymbol{\rho}_2$, and in equation 4.3 that is the case because it depends only on $\psi_{12}=\cos^{-1}(\hat{\mathbf{N}}_1\cdot\hat{\mathbf{N}}_2)$. But that is not the case in equation 5.3.

Contributions to the metric arising from changes in the misorientation relationship must be separated from those arising from changes in the mean boundary plane. Unless the rotation axis is normal to the boundary plane there will be changes to the boundary normals as a result of changes in the misorientation relationship. But those changes must not be double-counted by including them as a separate contribution to the metric arising from changes in the boundary normals. It

is a feature of equations 2.1 and 2.2 that this separation is explicit from the outset because the misorientation relation $\boldsymbol{\rho}$ and the mean boundary plane $\mathbf{N}$ are independent variables.

(b) Cahn and Taylor (2006)

Cahn and Taylor [11] expressed the view that in defining a metric there is no unique way of weighting the importance of the difference in misorientation between two grains with the difference in boundary normals. In this work the contribution to the metric of equation 4.3 from the change of the crystal misorientation is independent from the change of the mean boundary plane. As a result of their independence they must have an equal weighting: in general changes in both contributions are required to map one boundary onto another. In the previous subsection we showed that the metric of Morawiec [10] does not achieve this separation of the contributions. In the next section we show that the metric of Olmsted [12] does not either.

(c) Olmsted (2009)

Olmsted [12] introduced a metric that was expressed entirely in terms of rotations. Thus, Olmsted creates a grain boundary in the plane $z=0$ of a reference lattice by rotating the lattice in $z>0$ by a rotation $\boldsymbol{\rho}_A$, and rotating the lattice in $z<0$ by a rotation $\boldsymbol{\rho}_B$. The boundary is thus characterised by two rotations, $(\boldsymbol{\rho}_A, \boldsymbol{\rho}_B)$, which involves six degrees of freedom. Olmsted identifies the redundant degree of freedom with a common rotation of both grains about the boundary normal, which leaves the grain boundary invariant but alters the rotations $\boldsymbol{\rho}_A$ and $\boldsymbol{\rho}_B$. The misorientation between the lattices in the two half-spaces is $\boldsymbol{\rho}_{A\to B} = \boldsymbol{\rho}_B \star (-\boldsymbol{\rho}_A)$.

A second grain boundary may be characterized in a similar way by replacing $\boldsymbol{\rho}_A$ and $\boldsymbol{\rho}_B$ by $\boldsymbol{\rho}_C$ and $\boldsymbol{\rho}_D$ in $z>0$ and $z<0$ respectively: $(\boldsymbol{\rho}_A, \boldsymbol{\rho}_B) \to (\boldsymbol{\rho}_C, \boldsymbol{\rho}_D)$. Olmsted then defines the following metric, expressed in our notation:

$$d^2 = 8\,\frac{\boldsymbol{\rho}^2_{A\to C} + \boldsymbol{\rho}^2_{B\to D} + 2\boldsymbol{\rho}^2_{A\to C}\boldsymbol{\rho}^2_{B\to D}}{\left(1+\boldsymbol{\rho}^2_{A\to C}\right)\left(1+\boldsymbol{\rho}^2_{B\to D}\right)} \tag{5.4}$$

where $\boldsymbol{\rho}_{A\to C} = \boldsymbol{\rho}_C \star (-\boldsymbol{\rho}_A)$ and $\boldsymbol{\rho}_{B\to D} = \boldsymbol{\rho}_D \star (-\boldsymbol{\rho}_B)$. This metric should include the contributions from the change in the misorientation relation from $\boldsymbol{\rho}_{A\to B}$ to $\boldsymbol{\rho}_{C\to D}$ and the change in the mean boundary planes.

It is clear that $\boldsymbol{\rho}_{C\to D} \star \boldsymbol{\rho}_{D\to B} \star \boldsymbol{\rho}_{B\to A} \star \boldsymbol{\rho}_{A\to C} = \mathbf{0}$. The change in the misorientation relationship between the crystals is given by $\boldsymbol{\rho}_{C\to D} \star -(\boldsymbol{\rho}_{A\to B}) = \boldsymbol{\rho}_{C\to D} \star \boldsymbol{\rho}_{B\to A}$. It is not possible to express this in terms of only $\boldsymbol{\rho}_{A\to C}$ and $\boldsymbol{\rho}_{B\to D}$. If $\boldsymbol{\rho}_{A\to B} = \boldsymbol{\rho}_{C\to D}$ the two boundaries share the same misorentation, and the boundaries differ only in their mean boundary planes. In that case $\boldsymbol{\rho}_{A\to C} = \boldsymbol{\rho}_{A\to B} \star \boldsymbol{\rho}_{B\to D} \star (-\boldsymbol{\rho}_{A\to B})$, confirming that the angle between grains A and C is identical to the angle between grains B and D, as expected in this case.

The difference between the metrics in equations 4.3 and 5.4 may best be illustrated with two examples. Setting $\hat{\mathbf{n}}_z = [001], \boldsymbol{\rho}_A = -\boldsymbol{\rho}_B = \tan(\frac{1}{2}\tan^{-1}\left(\frac{1}{5}\right))[010]$, and $\boldsymbol{\rho}_C = -\boldsymbol{\rho}_D = \tan(\frac{1}{2}\tan^{-1}\left(\frac{1}{2}\right))[010]$, we generate symmetric [010] tilt boundaries with normals $[105]/[\bar{1}05]$ and $[102]/[\bar{1}02]$ respectively. The mean boundary plane normals are both [001] so the 'distance' between these boundaries is exactly equal to the difference in their misorientations, which is given by $2\tan^{-1}\left(\frac{1}{2}\right) - 2\tan^{-1}\left(\frac{1}{5}\right) \approx 30.51^\circ$ for which $\tan^2(\theta/2) = 9/121 \approx 0.074$. This is also the result of applying equation 4.2. The result of applying equation 5.4 is $d^2 \approx 0.282$.

In the second example consider two grain boundaries sharing the same misorientation $\boldsymbol{\rho} = \frac{1}{2}[110]$, with boundary plane normals $[312]/[132]$ and $[7\bar{1}2]/[336]$, for which $\boldsymbol{\rho}^2_{A\to C} = \boldsymbol{\rho}^2_{B\to D} = (\sqrt{756}-24)/(\sqrt{756}+24)$. The metric of equation 5.4 then gives $d^2 = (\sqrt{756}-24)/\sqrt{756} \approx 0.127$. On the other hand since the boundary misorientations are the same the 'distance' between the boundaries is the angle between their mean boundary planes, which is just $\cos^{-1} 10/(3\sqrt{14})$, for which $\tan^2\psi_{12} \approx 0.058$.

We conclude that Olmsted's metric does not appear to measure either the difference in misorientation between the crystal lattices adjoining two boundaries, or the change of their mean boundary planes.

(d) The no boundary problem

Cahn and Taylor [11] identified a problem when the boundary misorientation angle θ tends to zero. When it is zero there is no grain boundary, just a single crystal. If we consider two small angle boundaries with mean boundary planes $\mathbf{N}_1$ and $\mathbf{N}_2$, then as θ_1 and θ_2 tend to zero the metric in equation 4.3 tends to $\psi_{12} = \cos^{-1}(\hat{\mathbf{N}}_1 \cdot \hat{\mathbf{N}}_2)$. The 'no boundary problem' is that the metric tends to a finite value, i.e. ψ_{12}, when there is no grain boundary 1 or 2, and ψ_{12} may be as large as $\pi/2$.

As $\theta_1, \theta_2 \to 0$ and ψ_{12} remains finite the boundaries will comprise distinct sets of dislocations if $\mathbf{N}_1 \neq \mathbf{N}_2$, as shown by Frank [4] and Hirth and Lothe [13]. In that limit $\Delta_{12} \to \psi_{12}$ reflects this distinction. If $\theta_1 = 0$ and $\theta_2 = 0$ the finite value of the metric if $\psi_{12} \neq 0$ should be viewed as the result of the limit $\theta_1, \theta_2 \to 0$. Alternatively, one can simply exclude the case where the misorientation angles are zero because there is no grain boundary to discuss.

6. The influence of point group symmetry

(a) Equivalent specifications of a grain boundary

Point group rotational symmetry complicates the picture considerably, as we shall illustrate for a face centred cubic (FCC) crystal. There are 24 rotational symmetries in the point group: the identity, 6 of $\pi/2$ about $\langle 100 \rangle$, 3 of π about $\langle 100 \rangle$, 6 of π about $\langle 110 \rangle$ and 8 of $2\pi/3$ about $\langle 111 \rangle$. These rotational symmetries lead to 24 equivalent specifications of a plane (hkl), and a further 24 are obtained by taking their negatives. They are referred to collectively by using braces: $\{hkl\}$. Suppose we have a grain boundary and we wish to characterise its five degrees of freedom in terms of the mean boundary plane and Rodrigues vector. Let the boundary plane be parallel, at least locally, to planes of the type $\{hkl\}$ and $\{h'k'l'\}$ in the two crystals. There are up to $48 \times 48 = 2,304$ equivalent specifications of the boundary plane in the two crystals. After we adjust the lengths of the vectors $\mathbf{n} = \langle hkl \rangle$ and $\mathbf{n}' = \langle h'k'l' \rangle$ to be the same we may generate up to $2,304$ mean boundary plane normals $\mathbf{N} = (\mathbf{n} + \mathbf{n}')/2$.

Let the misorientation of the crystal lattices be described by a Rodrigues vector $\boldsymbol{\rho}$. Equation 2.4 must hold for each specification of the boundary parameters: $\mathbf{n} = \boldsymbol{\rho} \star \mathbf{n}' \star (-\boldsymbol{\rho})$. Let $\boldsymbol{\sigma}_i$ be the Rodrigues vector representing the i'th rotational symmetry of the FCC crystal. The 24 Rodrigues vectors representing the rotational symmetries in an FCC crystal are listed in Table 1. We may generate 24 equivalent specifications of the boundary from equation 2.4 as follows:

$$\begin{aligned} (\boldsymbol{\sigma}_i \star \mathbf{n} \star (-\boldsymbol{\sigma}_i)) &= (\boldsymbol{\sigma}_i \star \boldsymbol{\rho}) \star \mathbf{n}' \star (-\boldsymbol{\rho}) \star (-\boldsymbol{\sigma}_i) \\ &= (\boldsymbol{\sigma}_i \star \boldsymbol{\rho}) \star \mathbf{n}' \star -(\boldsymbol{\sigma}_i \star \boldsymbol{\rho}) \end{aligned} \tag{6.1}$$

The left hand side of equation 6.1 is one of 24 equivalent specifications of the plane normal $\mathbf{n}$. The Rodrigues vector $(\boldsymbol{\sigma}_i \star \boldsymbol{\rho})$ represents one of the 24 equivalent ways of specifying the misorientation between the crystals. It is necessary to consider only the 24 Rodrigues vectors with directions that fall within or on the standard stereographic triangle defined by the directions $[001]$, $[101]$ and $[111]$[5]. We call this set of 24 Rodrigues vectors the 'standard set'.

A vector $\mathbf{v} = [v_1, v_2, v_3]$ lies within or on the standard triangle provided $v_3 \geq v_1 \geq v_2$. If the direction of $(\boldsymbol{\sigma}_i \star \boldsymbol{\rho})$ is outside the standard triangle one evaluates the set of 24 equivalent

[5] In a stereographic projection of a cubic crystal there are 24 triangles bounded by $\langle 100 \rangle$, $\langle 110 \rangle$ and $\langle 111 \rangle$ poles in each of the upper and lower hemispheres. There is one of the 48 equivalent plane normals $\langle hkl \rangle$ within or on each triangle.

Rodrigues vectors $(\boldsymbol{\sigma}_i \star \boldsymbol{\rho} \star \boldsymbol{\sigma}_j)$, among which one, or its negative, will fall within or on the standard triangle. In that case equation 6.1 becomes

$$(\boldsymbol{\sigma}_i \star \mathbf{n} \star (-\boldsymbol{\sigma_i})) = (\boldsymbol{\sigma}_i \star \boldsymbol{\rho} \star (-\boldsymbol{\sigma_j})) \star (\boldsymbol{\sigma}_j \star \mathbf{n}' \star (-\boldsymbol{\sigma_j})) \star -(\boldsymbol{\sigma}_i \star \boldsymbol{\rho} \star (-\boldsymbol{\sigma_j})) \tag{6.2}$$

To summarise, there are 24 equivalent Rodrigues vectors within or on the standard triangle describing the misorientation between the two crystals. For each member $\boldsymbol{\rho}_i$ of this standard set the boundary plane normals $\mathbf{n}_i$ and $\mathbf{n}'_i$ are related by $\mathbf{n}_i = \boldsymbol{\rho}_i \star \mathbf{n}'_i \star (-\boldsymbol{\rho}_i)$. All three vectors $\boldsymbol{\rho}_i, \mathbf{n}_i$ and $\mathbf{n}'_i$ are expressed in the coordinate system of the median lattice. The mean boundary plane corresponding to each member of the standard set is then $\mathbf{N}_i = \frac{1}{2}(\mathbf{n}_i + \mathbf{n}'_i)$. The 24 equivalent descriptions of the boundary in the standard triangle are characterised by the 24 pairs $(\hat{\mathbf{N}}_i, \boldsymbol{\rho}_i)$, where the mean boundary plane normal is specified as a unit vector to emphasise that only its direction matters, and hence only two degrees of freedom are associated with it. The boundary plane normals $(\mathbf{n}_i, \mathbf{n}'_i)$ are obtained using $\mathbf{n}_i = \mathbf{N}_i - \mathbf{N}_i \times \boldsymbol{\rho}_i$ and $\mathbf{n}'_i = \mathbf{N}_i + \mathbf{N}_i \times \boldsymbol{\rho}_i$, where the mean boundary plane normal does not have to be a unit vector.

(b) Example 1: the (111) twin in an FCC crystal

Obviously, the Miller indices are $\{111\}$ type on both sides of the boundary plane, but they are not necessarily the same Miller indices on both sides. The misorientation may be specified as $\pi/3$ about $\langle 111 \rangle$. The Rodrigues vector representing this misorientation in the standard triangle is $\boldsymbol{\rho} = \frac{1}{3}[111]$. It is also obvious that if we choose the boundary plane normals to be the same $\mathbf{n} = \mathbf{n}' = [111]$, then $\mathbf{n} = \boldsymbol{\rho} \star \mathbf{n}' \star (-\boldsymbol{\rho})$. According to this description the twin boundary is a $\pi/3$ (111) twist boundary.

By applying the 24 rotational symmetries, as in equation 6.1, to $[111] = \frac{1}{3}[111] \star [111] \star \frac{1}{3}[\bar{1}\bar{1}\bar{1}]$ we generate 24 Rodrigues vectors and the associated pairs of boundary normals. Twenty three of these Rodrigues vectors lie outside the standard triangle, the 24th being the original $\boldsymbol{\rho} = 1/3[111]$. Equivalent Rodrigues vectors may be found inside or on the standard triangle using equation 6.2, together with the associated pairs of boundary normals. It is found that there are just seven distinct Rodrigues vectors in the standard triangle, which are repeated certain numbers of times to make up the 24. These seven characterisations of the boundary are listed in Table 2, together with their degeneracies. A further seven descriptions are generated by negating $\mathbf{n}$ and $\mathbf{n}'$. These 14 relationships $\mathbf{n} = \boldsymbol{\rho} \star \mathbf{n}' \star (-\boldsymbol{\rho})$ may be rotated into the other 47 stereographic triangles using equation 6.2, giving a total of 672 distinct but equivalent characterisations of the (111) twin in terms of $\mathbf{N}$ and $\boldsymbol{\rho}$.

Some comments about Table 2 are in order. We have already seen that the boundary may be described as a twist boundary. It may also be described as a tilt or mixed tilt and twist boundary. The $\boldsymbol{\rho} = 1/2[101], [101]$ and $\infty[112]$ Rodrigues vectors lie in the corresponding boundary planes: these are tilt boundary descriptions. The $\boldsymbol{\rho} = [102]$ and $[113]$ Rodrigues vectors are inclined to the corresponding boundary planes: they are therefore mixed tilt and twist boundary descriptions. This lack of uniqueness of the classification of the twin boundary as tilt, twist or mixed is well known and it applies to other boundaries.

Secondly, there are two Rodrigues vectors in Table 2 (and Table 1) which have infinite length and are written as $\infty[112]$ and $\infty[111]$. They represent rotations by π about $[112]$ and $[111]$. If $\boldsymbol{\rho}_2$ is a rotation by π then equation 2.3 is evaluated by taking the limit $|\boldsymbol{\rho}_2| \to \infty$:

$$\begin{aligned} \boldsymbol{\rho}_2 \star \boldsymbol{\rho}_1 &= \lim_{|\boldsymbol{\rho}_2| \to \infty} \frac{\boldsymbol{\rho}_1 + \boldsymbol{\rho}_2 - \boldsymbol{\rho}_1 \times \boldsymbol{\rho}_2}{1 - \boldsymbol{\rho}_1 \cdot \boldsymbol{\rho}_2} \\ &= \frac{\boldsymbol{\rho}_1 \times \hat{\boldsymbol{\rho}}_2 - \hat{\boldsymbol{\rho}}_2}{\boldsymbol{\rho}_1 \cdot \hat{\boldsymbol{\rho}}_2} \end{aligned} \tag{6.3}$$

It follows that $\boldsymbol{\rho}_2 \star \mathbf{v} \star -\boldsymbol{\rho}_2 = 2(\hat{\boldsymbol{\rho}}_2 \cdot \mathbf{n})\hat{\boldsymbol{\rho}}_2 - \mathbf{v}$, where $\mathbf{v}$ is an arbitrary vector, which is a well known result. If both $|\boldsymbol{\rho}_1|, |\boldsymbol{\rho}_2| \to \infty$ then taking the limit $|\boldsymbol{\rho}_1| \to \infty$ of equation 6.3 we obtain:

$$\boldsymbol{\rho}_2 \star \boldsymbol{\rho}_1 \rightarrow \frac{\hat{\boldsymbol{\rho}}_1 \times \hat{\boldsymbol{\rho}}_2}{\hat{\boldsymbol{\rho}}_1 \cdot \hat{\boldsymbol{\rho}}_2} \tag{6.4}$$

This is another well known result, namely that an arbitrary rotation by θ about an axis $\hat{\mathbf{a}}$ may be described as two successive rotations by π about axes separated by an angle $\theta/2$, and both axes perpendicular to $\hat{\mathbf{a}}$.

In Table 2 the mean boundary plane for the rotation by π about $[112]$ in the boundary plane is written as $[\bar{1}10]/\infty$. In this case the axis of the rotation by π is normal to $\mathbf{n}$ and $\mathbf{n}'$. The notation $[\bar{1}10]/\infty$ signifies that the direction of the mean boundary plane normal is along $[\bar{1}10]$, and that its magnitude tends to zero as the magnitude of the Rodrigues vector tends to infinity. The difference $\mathbf{n}' - \mathbf{n} = 2\mathbf{N} \times \boldsymbol{\rho} = [22\bar{2}]$ is finite, and therefore $|\mathbf{N}|$ must approach zero in a particular limiting way as $|\boldsymbol{\rho}| \rightarrow \infty$. If we write $\mathbf{N} = (\hat{\boldsymbol{\rho}}/(2|\boldsymbol{\rho}|)) \times (\mathbf{n}' - \mathbf{n})$ then $|\mathbf{N}| \rightarrow 0$ as $|\boldsymbol{\rho}| \rightarrow \infty$ and $2\mathbf{N} \times \boldsymbol{\rho}$ is identically equal to $\mathbf{n}' - \mathbf{n}$ in the limit $|\boldsymbol{\rho}| \rightarrow \infty$ because $\hat{\boldsymbol{\rho}} \cdot \mathbf{n} = \hat{\boldsymbol{\rho}} \cdot \mathbf{n}' = 0$. It is easy to show that equations 2.1 and 2.2 are also satisfied by this choice of $\mathbf{N}$.

Our final comment about Table 2 is that for each Rodrigues vector there is a different mean boundary plane. If the angle of rotation represented by a particular choice of Rodrigues vector is traced back to zero the boundary plane will become a plane in the perfect crystal, the normal to which is $\hat{\mathbf{N}}$. The lack of uniqueness of the mean boundary plane is a direct consequence of the lack of uniqueness of the rotation describing the boundary misorientation. The mean boundary plane normal and the Rodrigues vector conspire in equations 2.1 and 2.2 to give boundary plane normals that are of the same types $\mathbf{n} = \langle hkl \rangle$ and $\mathbf{n}' = \langle h'k'l' \rangle$.

(c) Example 2: A less special boundary

In this example we consider a boundary parallel to a $\{223\}$ plane on one side and $\{885\}$ on the other, and the misorientation is $2\tan^{-1}(\sqrt{29}/7) \approx 75.14^\circ$ about $\langle 234 \rangle$[6].

In order for $\mathbf{n}$ and $\mathbf{n}'$ to be related by a rotation the normal $\langle 223 \rangle$ is multiplied by 3 to give it the same length as $\langle 885 \rangle$. The first task is to find a pair of plane normals $\mathbf{n}, \mathbf{n}'$ equal to $\langle 669 \rangle, \langle 885 \rangle$ (or $\langle 885 \rangle, \langle 669 \rangle$), and a Rodrigues vector $1/7\langle 234 \rangle$ such that $\mathbf{n} = \boldsymbol{\rho} \star \mathbf{n}' \star (-\boldsymbol{\rho})$. There are 2,304 possible choices, and we need just one from which all the others may be generated by applying the symmetry rotations of Table 1.

One choice is $[696] = \frac{1}{7}[234] \star [858] \star \frac{1}{7}[\bar{2}3\bar{4}]$. Applying the symmetry rotation of π about $[1\bar{1}0]$ to this relationship it may be transformed into one involving a Rodrigues vector in the standard triangle: $[9\bar{6}\bar{6}] = \frac{1}{7}[3\bar{2}\bar{4}] \star [5\bar{8}\bar{8}] \star \frac{1}{7}[324]$. This may be expressed as $[588] = \frac{1}{7}[324] \star [966] \star \frac{1}{7}[\bar{3}\bar{2}4]$, for which the Rodrigues vector $\frac{1}{7}[324]$ lies in the standard triangle. This relationship is the first entry in Table 3.

The other 23 entries in Table 3 are obtained from the first by applying the rotational symmetries of Table 1 using equations 6.1 and 6.2 to generate equivalent relationships $\mathbf{n} = \boldsymbol{\rho} \star \mathbf{n}' \star (-\boldsymbol{\rho})$ with Rodrigues vectors in the standard triangle. A further 24 may be obtained by negating $\mathbf{n}$ and $\mathbf{n}'$ in Table 3. These 48 relationships between $\mathbf{n}$ and $\mathbf{n}'$ with $\boldsymbol{\rho}$ in the standard triangle may be rotated using equation 6.2 into 48 relationships in each of the other 47 stereographic triangles, thus generating 2,304 descriptions of the boundary in total. For each description the 5 degrees of freedom are $\boldsymbol{\rho}$ and the mean boundary plane normal $\mathbf{N}$, from which the boundary plane normals $\mathbf{n}$ and $\mathbf{n}'$ may be generated using equations 2.1 and 2.2. All 2,304 descriptions of this boundary have the rotation axis inclined to the boundary plane, and therefore they are all mixed tilt and twist boundary descriptions.

(d) The 'distance' between these two boundaries

Let the set of 672 characterisations of the (111) twin boundary be $\{\mathbf{N}_i^{(1)}, \boldsymbol{\rho}_i^{(1)}\}, i = 1, 2, 3, \ldots 672$. Let the set of 2,304 characterisations of the $\{669\}\{558\}$ boundary of the previous section be $\{\mathbf{N}_j^{(2)}, \boldsymbol{\rho}_j^{(2)}\}, j = 1, 2, 3, \ldots 2,304$. To change the boundary represented by $(\mathbf{N}_i^{(1)}, \boldsymbol{\rho}_i^{(1)})$ into the

[6]The associated coincidence site lattice is $\Sigma = 39b$

boundary represented by $(\mathbf{N}_j^{(2)}, \boldsymbol{\rho}_j^{(2)})$ the crystals have to undergo a change of misorientation represented by $\boldsymbol{\rho}_{ij}^{(1)\to(2)} = \boldsymbol{\rho}_j^{(2)} \star (-\boldsymbol{\rho}_i^{(1)})$, and the mean boundary plane has to undergo a change of orientation given by $\cos^{-1}(\hat{\mathbf{N}}_j^{(2)} \cdot \hat{\mathbf{N}}_i^{(1)})$. The 'distance' between the two boundaries is then the minimum value of $\Delta_{ij} = \cos^{-1}(\hat{\mathbf{N}}_j^{(2)} \cdot \hat{\mathbf{N}}_i^{(1)}) + 2\tan^{-1}\left|\boldsymbol{\rho}_{ij}^{(1)\to(2)}\right|$.

Without loss of generality we may limit the characterisations of the second boundary to the 24 listed in Table 3 in the standard triangle. It is found by inspection that each of the 24 misorientations represented in Table 3 is no more than $2\tan^{-1}(1/5) \approx 22.62^\circ$ from one of the misorientations listed in Table 2. Consider this set of 24 pairs of Rodrigues vectors in each of which the crystal misorientation changes by $2\tan^{-1}(1/5)$. The smallest Δ_{ij} is determined by the the smallest angle between the normals to the mean boundary planes, allowing for the possibility that either $\mathbf{N}$ may be negated. For $\boldsymbol{\rho}_j^{(2)} = \frac{1}{7}[324]$ and $\boldsymbol{\rho}_i^{(1)} = \frac{1}{3}[111]$ the normals to the mean boundary planes are both $[111]$. The 'distance' between these two boundaries is therefore $2\tan^{-1}(1/5) \approx 22.62^\circ$. The twin boundary with normals $\mathbf{n} = \mathbf{n}' = [111]$ and $\boldsymbol{\rho} = \frac{1}{3}[111]$ is transformed into the second boundary with normals $\mathbf{n} = [588], \mathbf{n}' = [966]$ and $\boldsymbol{\rho} = \frac{1}{7}[324]$ by applying the change of crystal misorientation represented by $\boldsymbol{\rho} = \frac{1}{15}[2\bar{1}2]$ i.e. $\frac{1}{7}[324] = \frac{1}{15}[2\bar{1}2] \star \frac{1}{3}[111]$, and the mean boundary plane does not change. Along this path the Rodrigues vector changes according to:

$$\boldsymbol{\rho}(\lambda) = \frac{1}{3}[111] + \frac{2\lambda}{45 - 3\lambda}[2\bar{1}5], \tag{6.5}$$

where λ varies from 0 to 1. For example, when $\lambda = \frac{1}{3}, \boldsymbol{\rho} = \frac{1}{22}[879], \mathbf{n} = [20\ 23\ 23], \mathbf{n}' = [24\ 21\ 21]$, and when $\lambda = \frac{2}{3}, \boldsymbol{\rho} = \frac{1}{43}[17\ 13\ 21], \mathbf{n} = [35\ 47\ 47], \mathbf{n}' = [51\ 39\ 39]$. Along this path $\mathbf{n} + \mathbf{n}'$ remains parallel to $[111]$.

We note that this shortest path does not involve the description of the $\{669\}\{558\}$ boundary in which the misorientation has the smallest angle – the so called disorientation relationship. The Rodrigues vector for the disorientation relation is $\frac{1}{8}[213]$ and the mean boundary plane is [14 11 17]. The change of mean boundary plane involves a rotation of $\approx 9.92^\circ$, in addition to the change of misorientation of $\approx 22.62^\circ$.

7. Discussion

In a triclinic crystal the task of finding the distance between two grain boundaries is relatively straightforward using equation 4.3. The boundary plane normals $\mathbf{n}$ and $\mathbf{n}'$[7] and the Rodrigues vector $\boldsymbol{\rho}$ must be related by equation 2.4. There is no ambiguity about the specification of these vectors because there are no rotational symmetries.

The existence of up to 2,304 equivalent specifications of a grain boundary in an FCC crystal makes the task much more complicated, as we have illustrated in section 6. As shown in section (a) there are up to 24 characterisations $\{(\mathbf{N}_i^{(b)}, \boldsymbol{\rho}_i^{(b)})\}$ of a grain boundary 'b' with equivalent Rodrigues vectors in the standard triangle. Each of them satisfies $\mathbf{n}_i^{(b)} = \boldsymbol{\rho}_i^{(b)} \star \mathbf{n}_i'^{(b)} \star (-\boldsymbol{\rho}_i^{(b)})$, where $\mathbf{n}_i^{(b)} = \mathbf{N}_i^{(b)} - \mathbf{N}_i^{(b)} \times \boldsymbol{\rho}_i^{(b)}$ and $\mathbf{n}_i'^{(b)} = \mathbf{N}_i^{(b)} + \mathbf{N}_i^{(b)} \times \boldsymbol{\rho}_i^{(b)}$. Given two boundaries $b = 1$ and $b = 2$ the distance between them is determined by the minimum value of $\Delta_{ij} = \cos^{-1}(\hat{\mathbf{N}}_i^{(1)} \cdot \hat{\mathbf{N}}_j^{(2)}) + 2\tan^{-1}\left|\boldsymbol{\rho}_{ij}^{(1)\to(2)}\right|$, where $\boldsymbol{\rho}_{ij}^{(1)\to(2)} = \boldsymbol{\rho}_j^{(2)} \star (-\boldsymbol{\rho}_i^{(1)})$. The minimum value does not necessarily involve the misorientation relationships with the smallest angles of misorientation, i.e. the disorientations.

Even the distance between boundaries sharing the same crystal misorientation needs care, as in the case of the embedded crystal. For example, consider an embedded FCC crystal in the $\Sigma = 3$ orientation with a surrounding FCC crystal. There are four boundaries parallel to $\{111\}$ in the embedded grain. One of them is the twin boundary $\{111\}$, the other three are parallel to $\{115\}$ planes in the surrounding crystal. What is the shortest distance between the twin and any one of the $\{333\}\{115\}$ facets? By inspecting the set of four boundaries found

[7] The normal to the plane (hkl) is along $h\mathbf{a}_1^* + k\mathbf{a}_2^* + l\mathbf{a}_3^*$ where the $\mathbf{a}_i^*$ are basis vectors of the reciprocal lattice.

with each of the seven equivalent misorientation relationships in Table 2 it is found that the smallest angle between the mean boundary planes of the twin and any one of the $\{333\}\{115\}$ facets is 29.21°. It is achieved with $\boldsymbol{\rho} = [113]$, between the twin $\mathbf{n}' = [\bar{1}11], \mathbf{n} = [1\bar{1}1], \mathbf{N} = [001]$, and the facet $\mathbf{n}' = [333], \mathbf{n} = [\bar{1}15], \mathbf{N} = [124]$. The path between these two boundaries is defined by equation 4.1 with $\hat{\mathbf{N}}_1 = [001], \hat{\mathbf{N}}_2 = \frac{1}{\sqrt{21}}[124], \sin\psi_{12} = \sqrt{\frac{5}{21}}$. Equations 2.1 and 2.2 enable $\mathbf{n}$ and $\mathbf{n}'$ to be calculated along this path using $\hat{\mathbf{N}}$ thus defined and $\boldsymbol{\rho} = [113]$. This example demonstrates that even when two boundaries share the same misorientation it is essential to consider the equivalent boundary misorientations to identify the smallest distance between their mean boundary planes. It is also another demonstration that the shortest path does not necessarily involve the disorientation relationship.

Data Accessibility. All the data in this paper is in the tables included in the paper.

Acknowledgements. The authors are grateful to Peter Haynes for critical comments on an earlier draft of this paper. Part of this research was undertaken as a fourth year undergraduate project in the Department of Physics at Imperial College, using departmental computing facilities.

Conflict of interests. The authors declare they have no conflicts of interest.

Authors' Contributions. EPB and ARW wrote computer programs that enabled the simplifications of equations 6.1 and 6.2 to be identified and tested. APS defined and led the research, created the geometrical constructions and all the figures and wrote the paper.

Funding. No research funding was sought or provided for this research.

References

1. A. P. Sutton and R. W. Balluffi (1995). *Interfaces in crystalline materials*, Oxford University Press: Oxford.
2. G. Herrmann, H. Gleiter and G. Bäro (1975). Investigation of low energy grain boundaries in metals by a sintering technique. Acta Metallurgica, **24**, 353-359.
3. A.P. Sutton and R. W. Balluffi (1987). On geometric criteria for low interfacial energies. Acta Metallurgica, **35**, 2177-2201.
4. F.C. Frank (1950). *Symposium on the plastic deformation of crystalline solids*, p.150. Office of Naval Research: Pittsburgh, Pennsylvania.
5. A.P. Sutton (1981). *The structure and properties of grain boundaries*. PhD thesis, The University of Pennsylvania.
6. A. P. Sutton and V. Vitek (1983). On the structure of tilt grain boundaries in cubic metals II. Asymmetrical tilt boundaries. Philosophical Transactions of the Royal Society of London Series A **309**, 37-54.
7. O. Rodrigues (1840). Des lois géométriques qui régissent les déplacements d'un système solide dans l'espace et de la variation des coordonnées provenant de ces déplacements considérés indépendamment des causes qui peuvent les produire. *Journal de Mathématiques Pure et Appliquées*, **5**, 380-440.
8. J. W. Gibbs (1931). Elements of Vector Analysis, paragraph 145 in *The Collected Works*, Volume 2, Longman, Green and Co.: New York. See also E. B. Wilson (1922), paragraph 127 in *Vector Analysis: A Text-Book for the Use of Students of Mathematics and Physics, Founded Upon the Lectures of J. Willard Gibbs*, Yale University Press: New Haven.
9. J.H. Conway and D. A. Smith (2003), *On quaternions and octonions*, A. K. Peters Ltd.: Natick Massachusetts.
10. A. Morawiec (2000). Method to calculate the grain boundary energy distribution over the space of macroscopic boundary parameters from the geometry of triple junctions. Acta Mater. **48**, 3525-3532.
11. J. W. Cahn and J. E. Taylor (2006). Metrics, measures and parametrizations for grain boundaries: a dialog. *J. Mater. Sci.*, **41**, 7669-7674.
12. D. L. Olmsted (2009). A new class of metrics for the macroscopic crystallographic space of grain boundaries. Acta Materialia **57**, 2793-2799.

13. J. P. Hirth and J. Lothe (1982). *Theory of dislocations*, 2nd edition. Krieger: Malabar, Florida. See p.703-721.

Table 1. Axis, angle and Rodrigues vectors for 24 rotational symmetries in FCC crystals and how they transform the components of [HKL].

Axis	Angle	Rodrigues vector	[HKL]→
⟨UVW⟩	0	**0**	[HKL]
[110]	π	∞[110]	[KH$\bar{\text{L}}$]
[1$\bar{1}$0]	π	∞[1$\bar{1}$0]	[$\bar{\text{K}}\bar{\text{H}}$L]
[101]	π	∞[101]	[L$\bar{\text{K}}$H]
[10$\bar{1}$]	π	∞[10$\bar{1}$]	[$\bar{\text{L}}\bar{\text{K}}\bar{\text{H}}$]
[011]	π	∞[011]	[$\bar{\text{H}}$LK]
[01$\bar{1}$]	π	∞[01$\bar{1}$]	[$\bar{\text{H}}\bar{\text{L}}\bar{\text{K}}$]
[100]	π	∞[100]	[H$\bar{\text{K}}\bar{\text{L}}$]
[010]	π	∞[010]	[$\bar{\text{H}}$K$\bar{\text{L}}$]
[001]	π	∞[001]	[$\bar{\text{H}}\bar{\text{K}}$L]
[111]	$2\pi/3$	[111]	[LHK]
[$\bar{1}\bar{1}\bar{1}$]	$2\pi/3$	[$\bar{1}\bar{1}\bar{1}$]	[KLH]
[11$\bar{1}$]	$2\pi/3$	[11$\bar{1}$]	[K$\bar{\text{L}}\bar{\text{H}}$]
[$\bar{1}\bar{1}$1]	$2\pi/3$	[$\bar{1}\bar{1}$1]	[$\bar{\text{L}}$H$\bar{\text{K}}$]
[1$\bar{1}$1]	$2\pi/3$	[1$\bar{1}$1]	[$\bar{\text{K}}\bar{\text{L}}$H]
[$\bar{1}$1$\bar{1}$]	$2\pi/3$	[$\bar{1}$1$\bar{1}$]	[L$\bar{\text{H}}\bar{\text{K}}$]
[$\bar{1}$11]	$2\pi/3$	[$\bar{1}$11]	[$\bar{\text{K}}$L$\bar{\text{H}}$]
[1$\bar{1}\bar{1}$]	$2\pi/3$	[1$\bar{1}\bar{1}$]	[$\bar{\text{L}}\bar{\text{H}}$K]
[100]	$\pi/2$	[100]	[H$\bar{\text{L}}$K]
[$\bar{1}$00]	$\pi/2$	[$\bar{1}$00]	[HL$\bar{\text{K}}$]
[010]	$\pi/2$	[010]	[LK$\bar{\text{H}}$]
[0$\bar{1}$0]	$\pi/2$	[0$\bar{1}$0]	[$\bar{\text{L}}$KH]
[001]	$\pi/2$	[001]	[$\bar{\text{K}}$HL]
[00$\bar{1}$]	$\pi/2$	[00$\bar{1}$]	[K$\bar{\text{H}}$L]

Table 2. The seven characterisations of the FCC (111) twin with misorientation axes in the standard triangle and their degeneracies. In each case $\mathbf{n} = \boldsymbol{\rho} \star \mathbf{n}' \star (-\boldsymbol{\rho})$. The boundary normals $\mathbf{n}$ and $\mathbf{n}'$ are related to the mean boundary normal $\mathbf{N}$ and the Rodrigues vector $\boldsymbol{\rho}$ through equations 2.1 and 2.2.

Rodrigues vector	$\mathbf{n}'$	$\mathbf{n}$	$\mathbf{N}$	degeneracy
$\frac{1}{3}$[111]	[111]	[111]	[111]	2
[102]	[1$\bar{1}$1]	[111]	[101]	6
∞[112]	[11$\bar{1}$]	[$\bar{1}\bar{1}$1]	[$\bar{1}$10]	3
[113]	[$\bar{1}$11]	[1$\bar{1}$1]	[001]	6
∞[111]	[111]	[111]	[111]	1
[101]	[11$\bar{1}$]	[$\bar{1}$11]	[010]	3
$\frac{1}{2}$[101]	[$\bar{1}$11]	[$\bar{1}\bar{1}$1]	[$\bar{1}$01]	3

Table 3. The twenty four characterisations of a grain boundary with plane $\{966\}/\{588\}$ and misorientation axes in the standard triangle equivalent to $2\tan^{-1}(\sqrt{29}/7) \approx 75.14^\circ$ about $\langle 234 \rangle$. In each case $\mathbf{n} = \boldsymbol{\rho} \star \mathbf{n}' \star (-\boldsymbol{\rho})$. The boundary normals $\mathbf{n}$ and $\mathbf{n}'$ are related to the mean boundary normal $\mathbf{N}$ and the Rodrigues vector $\boldsymbol{\rho}$ through equations 2.1 and 2.2.

Rodrigues vector	$\mathbf{n}'$	$\mathbf{n}$	$\mathbf{N}$
$\frac{1}{7}[324]$	$[966]$	$[588]$	$[111]$
$\frac{1}{5}[3\,1\,11]$	$[6\bar{6}9]$	$[588]$	$[11\,2\,17]$
$[5\,3\,11]$	$[\bar{6}9\bar{6}]$	$[88\bar{5}]$	$[2\bar{1}1]$
$\frac{1}{7}[519]$	$[9\bar{6}6]$	$[885]$	$[17\,2\,11]$
$[759]$	$[\bar{6}\bar{6}9]$	$[85\bar{8}]$	$[2\bar{1}1]$
$\frac{1}{3}[215]$	$[8\bar{5}8]$	$[696]$	$[747]$
$[325]$	$[\bar{5}\bar{8}8]$	$[96\bar{6}]$	$[2\bar{1}1]$
$\frac{1}{3}[427]$	$[\bar{6}69]$	$[8\bar{8}5]$	$[1\bar{1}7]$
$\frac{1}{2}[437]$	$[\bar{5}88]$	$[9\bar{6}6]$	$[217]$
$\frac{1}{4}[327]$	$[\bar{8}58]$	$[6\bar{9}6]$	$[\bar{1}\bar{2}7]$
$[546]$	$[669]$	$[858]$	$[14\,11\,17]$
$\frac{1}{8}[213]$	$[858]$	$[669]$	$[14\,11\,17]$
$\frac{1}{3}[218]$	$[\bar{6}69]$	$[5\bar{8}8]$	$[\bar{1}\,\bar{2}\,17]$
$\frac{1}{4}[516]$	$[\bar{8}5\bar{8}]$	$[9\bar{6}\bar{6}]$	$[1\,\bar{1}\bar{1}\,2]$
$[328]$	$[88\bar{5}]$	$[\bar{6}9\bar{6}]$	$[2\,1\,11]$
$\frac{1}{6}[415]$	$[88\bar{5}]$	$[\bar{6}9\bar{6}]$	$[2\,17\,1]$
$\frac{1}{2}[318]$	$[\bar{5}88]$	$[6\bar{9}6]$	$[1\,\bar{1}\,14]$
$\frac{1}{5}[416]$	$[96\bar{6}]$	$[\bar{8}85]$	$[1\,14\,\bar{1}]$
$\frac{1}{2}[315]$	$[6\bar{6}9]$	$[885]$	$[717]$
$\frac{1}{5}[213]$	$[9\bar{6}\bar{6}]$	$[5\bar{8}\bar{8}]$	$[71\bar{7}]$
$\frac{1}{5}[719]$	$[8\bar{5}8]$	$[966]$	$[17\,1\,14]$
$\frac{1}{9}[517]$	$[88\bar{5}]$	$[69\bar{6}]$	$[14\,1\,\bar{1}\bar{1}]$
$\frac{1}{3}[5\,1\,11]$	$[5\bar{8}8]$	$[696]$	$[11\,1\,14]$
$\frac{1}{11}[315]$	$[8\bar{5}\bar{8}]$	$[66\bar{9}]$	$[14\,1\,\bar{1}\bar{7}]$